communications earth & environment

Article

https://doi.org/10.1038/s43247-024-01721-z

Climate-driven interannual variability in subnational irrigation areas across Europe

Check for updates

Wanxue Zhu ✉ & Stefan Siebert

Irrigation profoundly impacts ecology and agricultural productivity, with irrigated areas varying across regions and years. Interannual dynamics of irrigation extent are lacking, particularly in humid regions of Europe. We analyzed the response of irrigated areas to drought conditions in areas equipped for irrigation and used the derived relationships to estimate annual irrigated areas for 32 European countries in the period 1990–2020. Interannual variability of irrigated areas varied notably, particularly in more humid Northern and Western Europe. In most humid regions, irrigated area is larger in dry years, whereas in more arid regions like Spain, it is larger in wet years. The largest irrigated area across Europe occurred in dry years 2003 and 2018 (11.93 and 11.77 million hectares), while the smallest is estimated for the wet years 2002 and 2014 (10.71 and 10.31 million hectares). The findings of this study help to improve scenario development and water resources management.

Irrigation is a major measure of land use intensification and is crucial for global food security[1–3]. In Europe, varying prevalence of irrigation exists, influenced by the environment, cropping pattern, socioeconomics, population, and water availability[4]. Mediterranean regions heavily rely on irrigation, accounting for 60–80% of total water withdrawal[5], while irrigation in Central and Northern Europe is supplementary to rainfall, accounting for less than 1% of total water abstractions[6]. In dry years irrigation is important for alleviating crop water stresses during critical crop phenological phases to ensure high productivity and meet crop quality requirements[7]. Agriculture faces considerable challenges under projected climate change such as increased temperature, shifting rainfall distribution, and more frequent and intensive extreme events like droughts, heat waves, and flooding[8]. These changes have already reduced water resources in some regions, exacerbated the vulnerability of agriculture, and widened the yield gap between irrigated and rainfed agriculture[9,10].

Water use for irrigation is determined by irrigation water volume required per unit irrigated area and irrigated extent. The former factor can be estimated by performing soil water balances and quantifying the water volume needed to ensure that crop evapotranspiration is at the potential level or a level minimizing drought impacts on crop yield[11]. Provided accurate climate, crop management, and soil property data, process-based models can effectively simulate variations in water use over time and space[6]. Survey data have indicated that the extent of irrigated cropland exhibits interannual variability, particularly in temperate zones, where varying climatic conditions necessitate different irrigation intensities during the crop-growing season[12]. However, understanding the dynamics in irrigated extent at large scales remains limited due to constraints in observations and investigations[5]. Accurately mapping irrigation areas is critical for managing water allocations, understanding water budgets, and improving model simulations[13–15]. Various global and continental irrigation extent databases exist from farm structure surveys, literature reviews, and multi-source remote sensing observations[5,16–21]. However, these datasets fail to capture the evolving irrigation patterns across Europe over extended periods, as they are often limited to specific locations, covering only single years or short periods. The most comprehensive database providing survey-based information is Eurostat[22–24], but it provides data only for the years when farm structure surveys or agricultural censuses were undertaken (about every three years). Such absence of up-to-date annual irrigation extent data hampers the analyses of historical and current water use patterns, as well as predicting the impact of projected future wet and dry conditions across Europe at an appropriate spatial scale.

Filling spatial and temporal gaps in irrigation extent data can be accomplished through three primary approaches: simple interpolation, process-based modeling, and remote sensing observations. Remote sensing combined with climate, land use, and crop cultivation information can map dynamic water use and irrigation extent by detecting variations in vegetation phenology, soil moisture, surface temperature, terrain, and elevation, or visually identifying irrigation features such as surface water bodies and center pivot schemes[19–21,25,26]. However, these methods come with considerable uncertainties and biases stemming from prior hypotheses, image classification strategies, and data sources, including issues like mixed pixels, misclassification, cloud cover, data scale transfer difficulties, and time lags between irrigation practices and actual observations[14,27,28]. In the context of these challenges, remote sensing is considered relatively accurate in arid and semi-arid regions[15,27,29], whereas for humid and temperate regions such as Western and Central Europe, results may deviate from ground surveys[2]. This is mainly due to the difficulties in detecting slight irrigation signals in humid areas, and the impacts of cloud cover on crop phenology detection.

Department of Crop Sciences, University of Göttingen, Von-Siebold-Str. 8, 37075 Göttingen, Germany. ✉e-mail: wanxue.zhu@agr.uni-goettingen.de

Moreover, Central and Eastern Europe underwent substantial changes in irrigation extent around 1990 due to political and socio-economic factors[30]. Unfortunately, the existing remote sensing products either do not cover long-time periods or have substantial limitations in accurately mapping irrigation in humid regions.

Simple interpolation is suitable for gap filling of time series for the area equipped for irrigation (AEI) due to its relative stability over short time periods. However, when dealing with the area actually irrigated (AAI), simple interpolation may not be suitable since it fails to account for the multifaceted factors affecting interannual variability in AAI such as the different benefits of using irrigation in dry and wet years. For example, in the Netherlands, the reported AAI was 62,190 hectares in the wet year 2002 but 202,260 hectares in the dry year 2006[24]. Little is known whether such observations can be generalized for other time periods and countries in Europe. Since the European farm structure surveys were not undertaken in the years 2003 and 2018, when large parts of Europe were affected by severe drought, it is also not known how much these droughts contributed to variations in AAI and how large total irrigated area has been in these years.

To improve the understanding of trends and interannual variability in the extent of irrigated land, this study addresses the following research questions: (1) What are the impacts of climate variability on the annual extent of irrigated land across Europe for the period 1990 to 2020? (2) How large is the difference of the irrigated area in wet and dry years across Europe? (3) How large are differences in the estimated irrigated area when considering the impacts of climate variability on irrigated area versus linear interpolation (simple approach) of observations? To answer these questions, we combined irrigation data collected by European-wide surveys with a crop drought indicator (CDI) simulated by the process-based global crop water model (GCWM)[31,32]. Irrigated area estimated by this advanced approach, will then be compared to those obtained via the simple approach of data points obtained from surveys and with independent datasets available for some specific years in the considered time period (Fig. 1).

Time series of areas equipped for irrigation

The total AEI of 32 countries had its maximum of 18.9 million hectares at the beginning of the time series in 1990, declined to a minimum of 15.7 million hectares in 2011, and increased later again to 16.7 million hectares by 2020 (Dataset 3 in Fig. 2). The regional hotspots of AEI remained consistent over this extended time period, but trends varied across regions (Supplementary A Fig. S1). In the first decade, a distinct pattern of AEI intensity (percentage of AEI to total area) emerged with a notable western increase, eastern decrease trend. For instance, Spain and France reported AEI increases of 41% and 30%, while Bulgaria and Germany experienced reductions of 74% and 57% (Fig. 2). During the second decade, AEI intensity changes were primarily concentrated in the Central and Eastern regions (Supplementary A Fig. S1). Apart from Poland, the countries in Eastern Europe continued to experience declining AEI intensity. In contrast, certain Central European areas like the northern Balkan Peninsula, witnessed slight increases, while AEI in other regions remained relatively stable. In the last decade, AEI exhibited a considerable increase in regions around 50–55°N

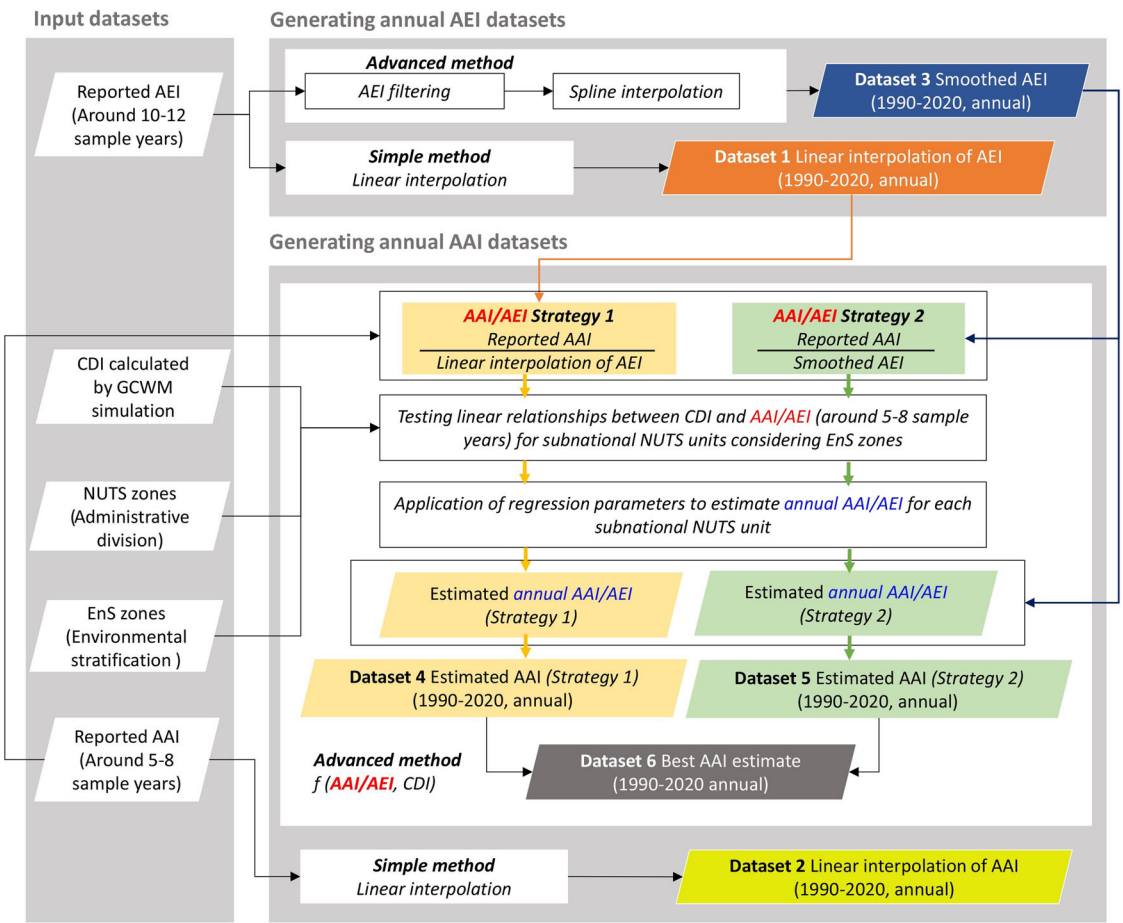

Fig. 1 | Scheme of generating European long-term irrigation area dataset (ELIAD). ELIAD provides subnational annual data on cropland areas equipped with irrigation infrastructure (irrigable area, AEI) and areas actually irrigated (AAI) for 32 European countries from 1990 to 2020. AAI/AEI × 100% is irrigation percentage, namely the fraction of AEI that is actually irrigated. GCWM is the global crop water model[32]. CDI is crop drought indicator calculated using actual and potential evapotranspiration simulated by GCWM[31]. EnS is the environmental stratification of Europe. Nomenclature of Territorial Units for Statistics (NUTS) is a statistical classification system; NUTS0 represents the national level, while the subnational levels in this study correspond to NUTS1 or NUTS2.

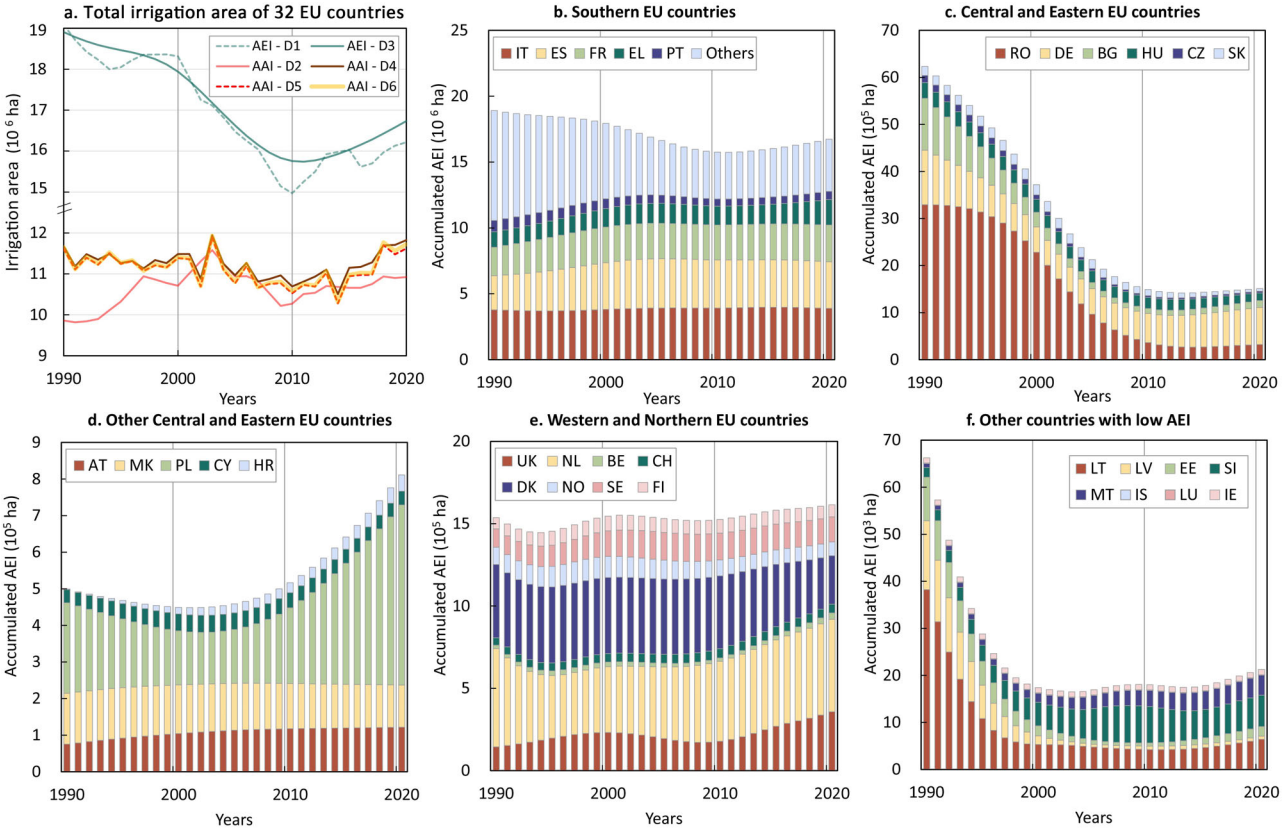

Fig. 2 | Total irrigation area of six ELIAD datasets in 32 European countries and national-level accumulated total AEI. a Total irrigation area of six ELIAD datasets in 32 European countries. Accumulated national-level total AEI of (**b**) Southern-, (**c**) Central and Eastern-, (**d**) Other Central and Eastern-, (**e**) Western and Northern-, and (**f**) Other (with low AEI) European (EU) countries. "Others" in (**b**) is the sum of AEI in other countries shown in (**c–f**). AEI data shown in (**b–f**) is from ELIAD Dataset 3. AAI and AEI are irrigated and irrigable area, respectively. D1–D6 represent Datasets 1–6 in ELIAD, and details for six datasets see the Data and Method section. Malta (MT) and Cyprus (CY) were not shown in the Southern European subfigure due to their small AEI values for better visualization.

and the eastern Balkan Peninsula. The Scandinavian Peninsula and northern Great Britain experienced decreases in AEI intensity, while other western and southern regions maintained stable AEI intensity. It is worth noting that most of the countries in Eastern Europe underwent AEI growth, distinguishing this decade from the previous two.

Impacts of drought conditions on the use of irrigation infrastructure

Linear regressions between CDI and reported irrigation percentage (100%×AAI/AEI, around 5–8 sample years) are developed for estimating annual irrigation percentage (Fig. 1). CDI emerges as a robust indicator for capturing irrigation area fluctuations, with correlation coefficients (r) between CDI and irrigation percentage between 0.50 and 0.75 for most regions (Fig. 3, $p < 0.05$). The strongest correlations are found for humid countries in Western Europe such as Belgium and the Netherlands, with positive r-values larger than 0.75 (Fig. 3d, e, $p < 0.05$), indicating that irrigation percentage is higher in dry years. In Central and Eastern European regions like Bulgaria, Slovakia, and Hungary, CDI-irrigation percentage correlations are weaker (0.50–0.75, Fig. 3b, c, e), likely because other factors than climate contributed considerably to AAI variability. Here, agricultural economic water scarcity often stems from socioeconomic and political factors rather than physical water scarcity[33,34]. Mediterranean regions exhibit generally weaker CDI-irrigation percentage correlations than temperate regions, particularly at the national level (Fig. 3a, e). Water scarcity, a primary driver in the Mediterranean, prompts adaptations frequently impacting water utilization and resources, and agricultural practices[5,35]. Spain and France show lower r-values at the national level, potentially influenced by their extensive geographical coverage across multiple climatic zones. Notably, we found negative CDI-irrigation percentage correlations for Spain, Cyprus, and Malta (Fig. 3a), possibly due to higher blue water scarcity, constraining the use of irrigation in dry years. Besides, CDI and irrigation percentage correlations are stronger when using smoothed AEI time series for Denmark, Finland, and Hungary but stronger when using reported AEI for Bulgaria, Switzerland, and Austria (Fig. 3a–d), therefore no clear preference can be determined for the superior method - using reported or smoothed AEI for calculating irrigation percentage (details about irrigation area data generation are in Data and Method, Fig. 1).

AAI in dry and wet years and AAI differences using two approaches

Considering the trends in AEI and the impacts of drought on the irrigation percentage, areas actually irrigated in the period 1990–2020 are estimated (Fig. 1). The largest AAI was estimated for the dry years 2003 (11.93 million ha) and 2018 (11.77 million ha) (Dataset 6, Fig. 4a, b). These years are characterized by drought in Central- and Western Europe and relatively wet conditions in Southern Europe (except for northern Italy in 2003, Fig. 5). The 2003 heatwave is considered a severe event in European recent history, while strengthened circulation patterns in 2018 caused drought in Central and Northern Europe[36]. AAI showed positive anomalies in particular in the drought-affected regions in Western- and Central Europe (Fig. 5c, d). AAI across the whole study region was smallest in the wet years 2002 (10.71 million ha) and 2014 (10.31 million ha) (Fig. 4a, b). These two years are wet years in most parts of Europe except the Baltic region (2002) and Spain (2014). AAI clearly shows negative anomalies in most of the regions affected by wetness in the growing season (Fig. 5a, b).

Differences in estimated AAI using the two approaches (Fig. 1) are more noticeable in temperate and Northern European regions than in

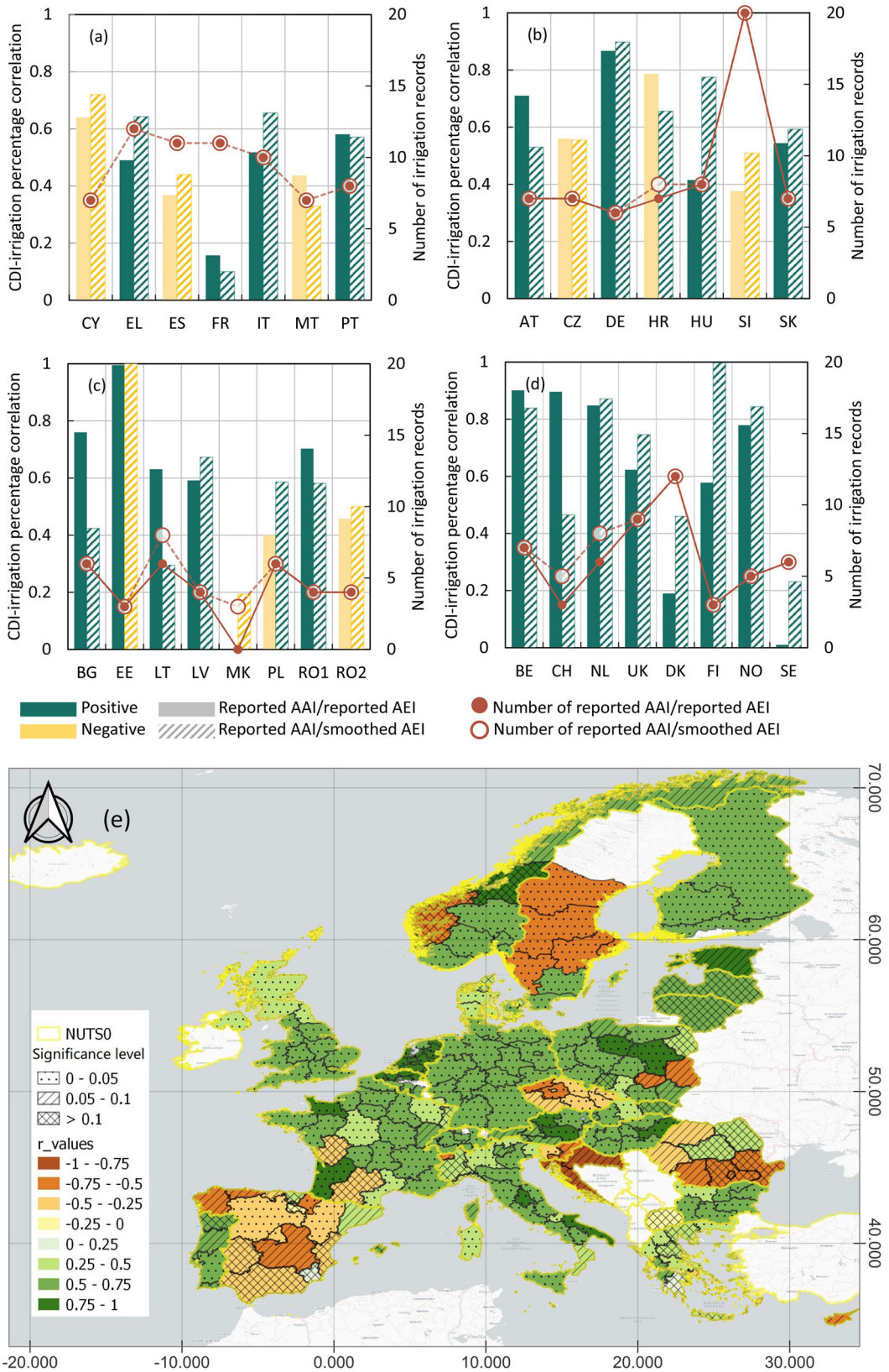

Fig. 3 | Pearson correlation coefficients (*r* values) between CDI and irrigation percentage at the national and subnational levels for 29 European countries. **a** Southern-, (**b**) Central-, (**c**) Eastern-, and (**d**) Western and Northern European countries at the national level, and (**e**) for the entire study region at the subnational level with significance levels. Data selected for creating ELIAD Dataset 6 is shown in (**e**). RO1 and RO2 represent two time periods for Romania, i.e., before 2010 and after 2010; subnational data for Romania is shown only for the RO2 period. Details for irrigation area datasets are explained in the Data and Methods section and Fig. 1. Country abbreviations are shown in Supplementary A Table S1. Only 29 countries are shown, because the AAI in Iceland is set as constant at 50 hectares, while no AAI data for Luxembourg (LU) and Ireland (IE).

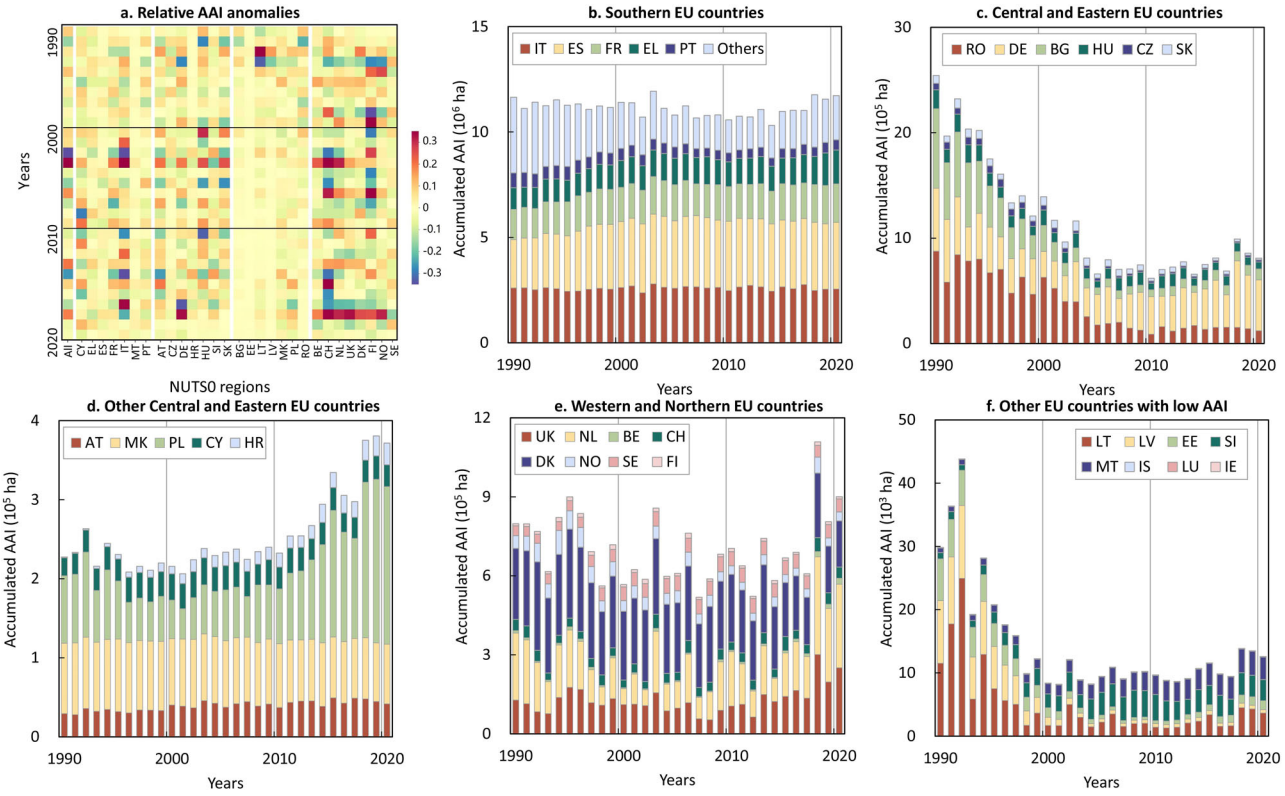

Fig. 4 | Relative AAI anomalies and accumulated AAI across 29 European countries. a Relative AAI anomalies in 29 European countries at the national level. Accumulated national level total AAI of (**b**) Southern-, (**c**) Central and Eastern-, (**d**) Other Central and Eastern-, (**e**) Western and Northern-, and (**f**) Other (with low AAI) European (EU) countries. AAI data is from ELIAD Dataset 6 which is considered our best guess. Details for calculating the relative AAI anomalies are in the Data and Methods section. "Others" in (**b**) is the sum of AAI in other countries shown in (**c**–**f**). no AAI data for Luxembourg (LU) and Ireland (IE). Malta (MT) and Cyprus (CY) were not shown in the Southern European subfigure due to their small AAI values for better visualization.

Mediterranean regions (Fig. 6). Specifically, Spain and Italy exhibit the smallest differences in estimated AAI between the two interpolation methods, while the United Kingdom (UK) and the Netherlands show large AAI differences. The advanced approach considering the impact of dry and wet conditions on irrigation percentage exhibited more interannual variability in AAI compared to the simple approach.

Irrigation percentage and differences between AAI and AEI time series

The subnational linear regression slope of 0.87 confirms the reliability of the estimated irrigation percentage in reflecting reported information, while the low R^2 is primarily due to biases in Eastern and Western Europe (Supplementary A Fig. S2). Over three decades, the coefficients of dispersion (CV_{MnAD}, Table 1)[37] for AEI in Southern and Northern Europe ranged from 2–16% (excluding Malta), but 5–19% in the humid temperate regions of Western Europe. In contrast, many countries in Central and Eastern Europe showed considerable AEI dispersion in the study period, even over 100% (Table 1). This strong variability in AEI affected total AAI in these regions as well and contributed more to the total variability of AAI in the study period than year-to-year variations caused by distinct climatic conditions (Fig. 4c). The spatial and temporal patterns of AAI closely aligned with AEI (Supplementary A Figs. S1 and S3), but AAI demonstrated more noticeable interannual fluctuation as indicated by CV_{MnAD} (Table 1). The average irrigation percentage across the study region was 65%, with South Europe showing the highest AAI and irrigation percentage (62%–89%), whilst modest AAI dispersion (≤ 15%, excluding Malta). Spain stands out with the highest irrigation percentage of 89%. The Eastern region, strongly influenced by trends in AEI, exhibited the most substantial AAI dispersion (can be over 100%). Notably, Northern and Western regions showed high AAI dispersion values (10%–50%), while their AEI dispersion coefficients were less pronounced (5%–20%), suggesting a considerable impact of climate on actual irrigation there.

Discussion

Our findings show that in most parts of Europe, the percentage of AEI that is really being used for irrigation varies considerably between years with higher irrigation percentages in dry years. This means that drought has a double effect on irrigation water requirements: increased irrigation water requirement per hectare of irrigated land and increased extent of irrigated land. Assessments ignoring the impact of drought on irrigated area will therefore underestimate irrigation water requirements in dry years considerably, in particular in Western-, Central-, and Northern Europe with increases of AAI of more than 35% in dry years (Fig. 4). A quantification of this effect will only become possible when gridded time series of the extent of irrigated crops become available.

Due to the limited availability of irrigation data, we used all records to generate the dynamic irrigation area dataset. Assessment is achieved by comparing our datasets with independent data, including Land Use/Cover Area frame statistical Survey (LUCAS) and remote sensing products (see Data and Methods). Datasets using the advanced approach and farm structure survey results (Fig. 1) exhibited moderate agreement of the irrigation percentage with results of the independent LUCAS survey (Fig. 7). Despite good agreement in Western (except for Sweden and the UK in 2018) and Mediterranean regions, irrigation percentage was larger in our dataset compared to observations in LUCAS for Central and Eastern Europe, revealing anomalies in these regions like Poland and Bulgaria. This difference may be caused by the specific setup of the LUCAS campaign in which sites are visited only once per year, potentially missing irrigation events in other periods of the season. Farm structure surveys provide a more comprehensive view of year-round irrigation practices. Mediterranean areas

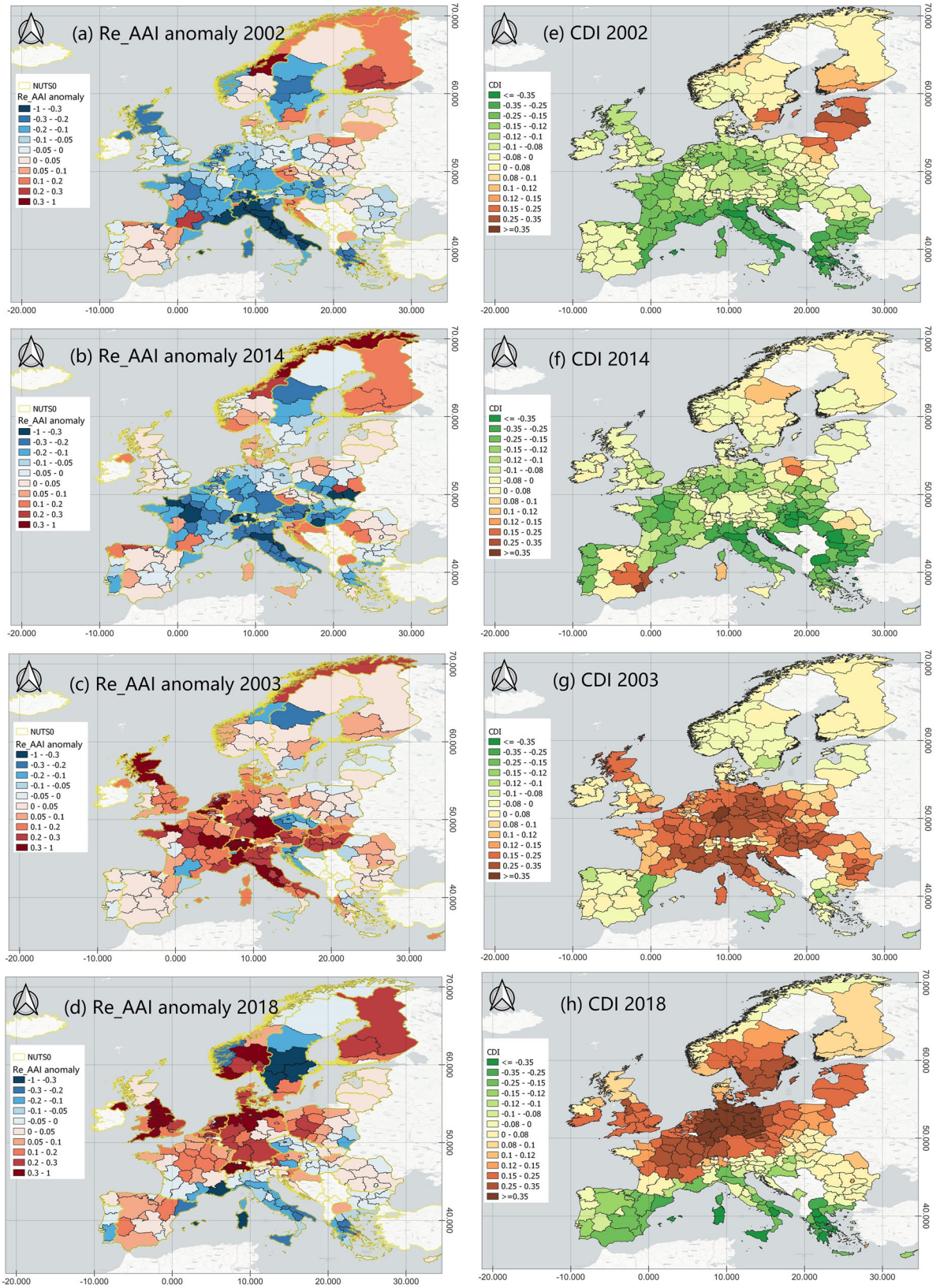

Fig. 5 | Subnational relative AAI anomalies and CDI values for wet and dry years in Europe. Subnational relative AAI anomalies in the years (**a**) 2002, (**b**) 2014, (**c**) 2003, and (**d**) 2018. Subnational CDI in the years (**e**) 2002, (**f**) 2014, (**g**) 2003, and (**h**) 2018. These four years are identified from the anomalies of relative AAI in Fig. 4a. Years 2002 and 2014 are identified as wet years, while 2003 and 2018 are identified as dry years for Europe. Red indicates the AAI in a specific year is higher than the expected AAI from the AAI smooth trendline, while blue indicates the lower conditions in (**a**–**d**). AAI is from the ELIAD Dataset 6. CDI in green indicates the specific year is wetter than the long-term reference year (1986–2015), while CDI in orange indicates dryer conditions.

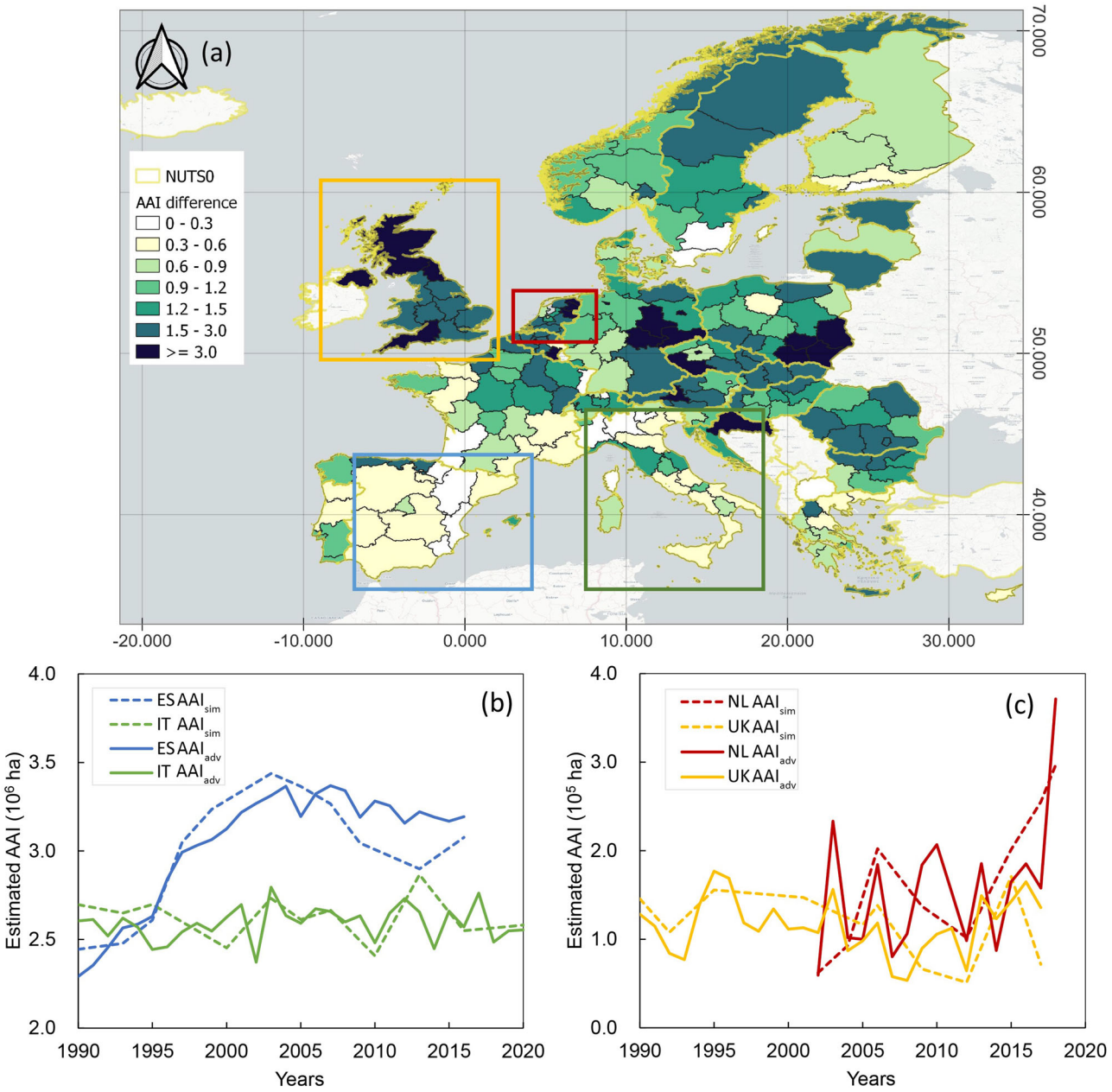

Fig. 6 | Differences of AAI using simple and advanced methods and AAI in two countries with high and low differences. a Differences of AAI using simple (ELIAD Dataset 2) and advanced (ELIAD Dataset 6) methods at subnational levels in Europe. Estimated AAI using simple and advances methods for (**b**) Spain (ES) and Italy (IT) with low AAI differences, and (**c**) the Netherlands (NL) and the United Kingdom (UK) with high AAI differences. The AAI difference for each subnational region is calculated as $\sqrt{\sum_{i=1}^{n}\left(AAI_{sim\,i}-AAI_{adv\,i}\right)^2}/[0.5\times(\overline{AAI_{sim}}+\overline{AAI_{adv}})]$; darker green indicates higher values, signifying higher disparities in estimated AAI between simple (AAI_{sim}) and advanced (AAI_{adv}) approaches; i is the sequence of year; excluded are AAI estimated using extrapolation, and specific time periods for AAI differences calculation are detailed in Supplementary A Table S1.

necessitate regular irrigation due to hot and arid climates[38], promoting the transition to fixed and efficient irrigation systems like drip irrigation, readily documented during on-site surveys. In contrast, the Eurostat 2010 survey found over 90% of Bulgarian farmers predominantly utilized surface irrigation, characterized by substantial water requirements. Such infrequent irrigation application is often underrepresented in one-time on-site surveys. Notably, the 2018 irrigation solely derived from our estimate without farm structure surveys, closely aligns with LUCAS data for most countries (1:1 line, Fig. 7), affirming the reliability of our datasets in most European regions.

The comparison to the remote sensing GIAM (Global Irrigated Area Map) (2000) product in AAI intensity revealed a considerable difference (Supplementary A Figs. S4 and S5). GIAM exhibited higher AAI intensity in countries like the Netherlands and Romania, possibly due to neglecting the irrigation fraction within each pixel, especially in areas with mixed features like fragmented farmlands and forests due to the coarse spatial resolution of the imagery[16,39,40]. The comparison to GRIPC (Global Rain-fed, Irrigated, and Paddy Croplands) (2005)[19] showed high consistency, while our data can detect smaller irrigation areas in Central and Eastern Europe. GMIE (Global Maximum Irrigation Extent) omitted regions with high irrigation intensity like parts of France and the Iberian Peninsula, due to the exclusion of permanent and fodder crops[21]. Overall, various datasets effectively identify irrigation hotspots. However, remote sensing has limited capability in detecting irrigation in Central and Eastern Europe, whereas the AAI in Western Europe shows noticeable discrepancies compared to our dataset. Remote sensing products, commonly derived from thermal, optical, and

Table 1 | Summary of irrigation extent of each country for the period 1990–2020

Regions	NUTS0	TA (10^3 ha)	Mean AEI (10^3 ha)	Mean AAI (10^3 ha)	Mean AAI/ Mean AEI	AEI CV_{MnAD} (%)	AAI CV_{MnAD} (%)	Irrigation contribution (%)
All	-	488942	17112	11143	65.1	5.9	2.7	51.2
Southern	CY	924	42	29	70.5	7.4	7.7	75.5
	EL	13183	1437	1211	84.3	8.8	8.6	64.1
	ES	50602	3432	3052	88.9	6.4	6.6	64.1
	FR	63837	2630	1641	62.4	3.4	4.9	36.6
	IT	30068	3866	2592	67.0	2.0	2.8	38.4
	MT	32	2.6	2.3	86.9	36.4	36.5	76.0
	PT	9200	673	520	77.3	15.8	14.8	65.8
Western	BE	3066	26	8.0	31.2	15.7	48.2	15.3
	CH	4129	52	37	70.6	5.4	17.4	3.2
	NL	3551	466	167	35.9	11.8	36.0	15.4
	UK	24481	221	129	58.3	18.9	30.0	25.9
Central	AT	8393	108	39	36.5	9.7	12.7	25.2
	CZ	7888	77	36	46.6	73.4	77.0	21.1
	DE	35777	685	372	54.4	17.7	24.6	24.6
	HR	5663	22	14	61.1	38.9	38.2	33.6
	HU	9302	253	109	43.1	14.6	23.1	35.6
	SI	2027	6	2.7	49.2	23.1	27.3	10.1
	SK	4903	158	52	32.7	25.8	35.4	31.1
Northern	DK	4311	428	258	60.3	7.0	11.9	9.5
	FI	33796	83	11	13.2	4.7	25.4	9.3
	IS	10266	0	0	-	-	-	-
	NO	32393	108	47	43.3	13.2	27.5	7.6
	SE	44991	150	48	32.3	8.4	10.8	17.0
Eastern	BG	11098	329	214	64.9	144	142	39.7
	EE	4537	3	1.9	71.8	103	105	12.4
	LT	6490	9	4.8	55.4	76.5	100	12.2
	LV	6460	3	2.3	83.7	326	333	16.7
	MK	2544	128	83	64.9	5.3	5.1	49.2
	PL	31192	233	80	38.6	36.4	45	20.5
	RO	23839	1482	369	24.9	112	109	40.0

The total area (TA) in each country is derived from NUTS2010 data in Eurostat. AAI is area actually irrigated. AEI is area equipped for irrigation. AAI/AEI is irrigation percentage, calculated by the percentage of AAI to AEI. AAI is from our generated European Long-term Irrigation Area Dataset (ELIAD), Dataset 6; AEI is from ELIAD Dataset 3. CV_{MnAD} is the coefficient of dispersion based on the mean absolute deviation around the median (MnAD)[37]; A high CV_{MnAD} value indicates a high degree of dispersion. The irrigation contribution is calculated by $CWU_B/(CWU_B + CWU_G)$, representing the mean contributions of irrigation to total crop water requirement; CWU_G and CWU_B are green and blue water use (m^3) of irrigated crops using the global crop water modeling[31,32], respectively. NUTS0 codes are described in Supplementary A Table S1.

microwave data, encounter challenges in capturing irrigation in regions with diverse crop development stages, especially in areas with mixed crop types and lush natural vegetation with humid climates[15,41]. Thermal information is less responsive to irrigation signature in humid regions due to reduced evaporative demands. Microwave sensitivity decreases with slight soil moisture differences in rainfed and irrigated cropland, particularly in areas with drip irrigation and proximity to water bodies[27].

Explaining differences between reported AAI data and estimated cropland area actually irrigated is challenging. These differences are attributed to data collection methodologies, objectives, and the potential for systematic over- and underresporting[39,42]. For instance, potential reasons for differences include consideration of water availability in defining AEI for Austria, and average conditions for the period 2008–2010 used in the Poland 2010 Agricultural Census. Reported irrigation data show differences in data availability, with Southern Europe having extensive records, while central and northern regions face limited information; pre-2000 data scarcity amplifies uncertainties regarding earlier periods. Regarding the irrigation reference period, we assumed July and August as high-irrigation months to alleviate dry and hot conditions experienced by crops, excluding irrigation for winter crops. Determining irrigation reference years is challenging in countries with surveys conducted in June and early July, such as Slovenia, Poland, Norway, and the UK. Testing different reference years (Supplementary B) helps alleviate potential uncertainties. Besides, data filtering has been made for evident outliers in reported data (Fig. 1), like abrupt variations in AEI values for the UK in Eurostat (Supplementary Data C1).

Three main factors in our advanced approach affect AAI estimation (Fig. 1). AEI filtering thresholds and smoothing are crucial since AAI estimation relies on correlations of CDI with irrigation percentage. AAI trend is determined by AEI, whilst CDI influenced interannual variations of AAI. However, CDI has inherent uncertainties and limitations stemming from input data sources, model structure, and assumptions made in the GCWM[32]. Notably, CDI calculation relies on static irrigated and rainfed crop information in MIRCA2000 (global Monthly Irrigated and Rainfed Crop Area around the year 2000) dataset[17], introducing uncertainties for characterizing climate conditions over the extensive time period, during

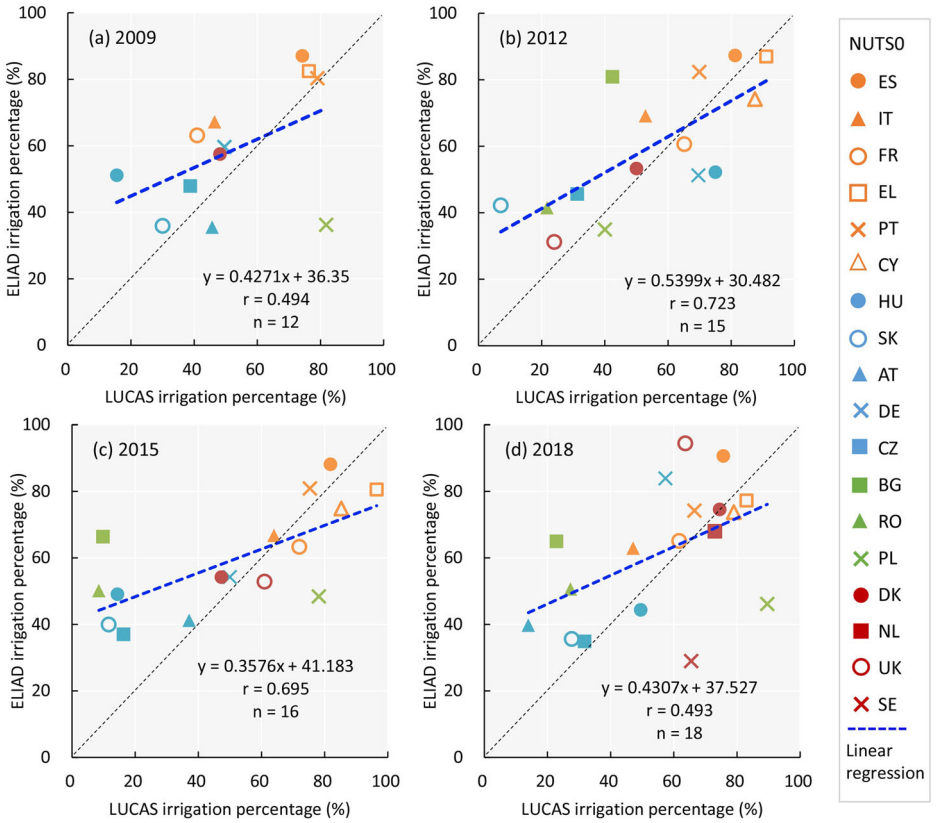

Fig. 7 | Irrigation percentage comparison between LUCAS and ELIAD datasets. Data comparison in the years (**a**) 2009, (**b**) 2012, (**c**) 2015, and (**d**) 2018. The irrigation percentage (AAI/AEI × 100%) is calculated by the percentage of AAI using the advanced approach (ELIAD Dataset 6) to smoothed AEI (ELIAD Dataset 3); calculations of LUCAS irrigation percentage see the Data and Method section.

which the changes of crop cultivation, patterns, and extents due to various factors like urbanization, economic development, political influences, and climate change[10,43,44]. A potential improvement is allocating reported irrigation extent to different crops, and then filling temporal irrigation gaps based on continuous crop cultivation information, but this requires large effort and introduces new uncertainties related to disaggregation strategies and crop cultivation extent. The SPAM (Spatial Production Allocation Model) dataset provides global crop-specific irrigation area approximately every 5 years since 2000[45]; however, its irrigation information is derived from GMIA v5.0 (Global Map of Irrigation Area) AEI data with a fixed reference year of 2005. Lastly, data from some regions with the same environmental condition (EnS zone[46]) or upper-level administrative unit are aggregated to establish more robust correlations between CDI and irrigation percentage when irrigation information of individual regions is insufficient, so AAI estimation is influenced by expert comprehensive judgment applied to the data aggregation from subnational regions (Supplementary Data C2). Determining the best aggregation strategy is challenging, especially when multiple eligible subnational regions exist.

We consider in our study the impact of climate on irrigation percentage. Nevertheless, irrigation percentage is influenced by various other factors, and climate importance may change over time and across regions. Freshwater availability is the prerequisite, and regions heavily reliant on irrigation may face a high probability of water scarcity resulting from severe or frequent drought[10]. Irrigation decision-making is dynamic, influenced by crop rotations, fallow periods, climate variability, and economic factors; rising crop prices often drive farmers to expand irrigation for better yields[15,47]. Besides, farm size, infrastructure development, innovations in crop cultivation and irrigation systems, and subsidy policies also play roles in water management[35,48]. Nonetheless, climate conditions display strong correlations with irrigation percentages in temperate regions. This bolsters the credibility of our datasets in such humid regions where other approaches such as remote sensing observations have usually posed considerable challenges.

Data and Methods

AEI (in hectares) is the extent of agricultural land and pastures (excluding kitchen gardens and crops under greenhouses) equipped with irrigation systems, regardless of actual irrigation practices; AAI (in hectares) is the area that received artificial water supplies at least once a year to alleviate drought stress. The irrigation percentage (0–100%) is the percentage of AEI that is actually irrigated (100%×AAI/AEI). Irrigation intensity is the percentage of the total area of a specific region that is irrigable or irrigated.

The European long-term irrigation area dataset (ELIAD, Supplementary Data D) generated in this study is referred as the dynamic dataset, emphasizing its superior temporal resolution (annual) compared to the majority of current irrigation area datasets which are typically updated every 3–5 years or refer to specific years. The main input data include AAI and AEI primarily reported by Eurostat[22–24] (denoted as reported AAI and AEI, about 5–12 sample years), annual CDI computed with GCWM[31,32], the Environmental stratification of Europe (EnS), and nomenclature of territorial units for statistics (NUTS) zones[49] (Fig. 1). Data processing followed the NUTS zones from Eurostat (Supplementary A Fig. S6), same as the classification standard of reported irrigation data. Specifically, all data were initially segregated by country (NUTS0), followed by the processing for each subnational unit within each country. For the UK, Germany, and Ireland, data were processed at the NUTS1 level due to limited data availability; while for all other countries, data were processed at the NUTS2 level. NUTS1 and NUTS2 are referred to as subnational levels (239 subnational units in total). Considering data availability, 32 European countries assigned to five regions are included in ELIAD (Supplementary A Table S1). EnS is employed to categorize subnational units into 13 zones based on climate and topography conditions[46]. Details on EnS determination for each subnational unit are in Supplementary A Fig. S6. The EnS and NUTS classifications aim to aggregate data from subnational units with similar environmental conditions or the same upper-level administrative unit to establish robust CDI-irrigation percentage correlations, when their individual reported irrigation information is insufficient. This data aggregation strategy was based on

expert judgment, comprehensively considering the correlation coefficients and significance levels between CDI and irrigation percentage (details are in Supplementary Data C2).

The generation of dynamic AAI and AEI datasets utilized both simple and advanced approaches (Fig. 1). The simple approach employed linear interpolation to fill in temporal gaps in reported AEI and AAI, resulting in Datasets 1 and 2, respectively. Dataset 3 (smoothed AEI) was produced using the advanced approach, which entailed filtering reported AEI and subsequently applying spline interpolation to the filtered AEI. The dynamic AAI generated by using the advanced approach relied on the time-series of AEI, and linear regression between CDI and irrigation percentage. Two strategies were implemented for calculating irrigation percentage, resulting in Datasets 4 and 5. The best guess of AAI estimate from Datasets 4 and 5 created Dataset 6. Datasets 1 and 2, generated by using the simple approach, adhered completely to the available reported values, while the other four datasets produced using the advanced approach exhibited partial disparities from the reported data.

Irrigation area data sources

The AAI and AEI data, primarily originate from Eurostat (accessed on March 10, 2023), national official statistics, historical irrigation dataset[18], and FAO Aquastat (accessed on July 01, 2023). Eurostat data is prioritized for its consistency and extensive records from farm structure surveys. If Eurostat data is unavailable, other datasets are utilized. When discrepancies arise between Eurostat and alternative sources, priority is given to Eurostat provided it does not exhibit conspicuous errors. For example, the AEI values for 2009 from Croatia national statistics (5219 ha) did not align with those provided by Eurostat (14490 ha). However, in subsequent years like 2012 and 2015, Eurostat reported AEI values of 13430 ha and 16070 ha, respectively, so we utilized the Eurostat data for 2010. In the case of the UK, AAI and AEI reported by Eurostat for the year 2002 were identical, indicating an irrigation percentage of 100%. Considering data from other years, we retained these values for AEI. Besides, Irrigation data are reported in Eurostat in intervals of two or three years, with considerable data gaps before 2000, especially for AAI. Specific sources of reported irrigation data for each region are detailed in Supplementary A Tables S2 and S3, and details of data processing are in Supplementary C. For consistency in time-series comparison, the NUTS2010 regional subdivision was used for mapping.

The reference periods of reported irrigation data were defined based on the information contained in the metadata of the farm structure surveys (Supplementary A Table S4, Supplementary B). For regions where irrigation information was recorded 12 months before the survey date, we assumed that irrigation practices primarily occurred during crop growing periods highly susceptible to drought or heat events, particularly in July and August. For example, in the case of Germany, farm structure survey data reported for 2010 captured irrigation practices in the period 12 months before May 2010, so the reference year for Germany was set to 2009 instead of 2010. For countries where surveys were conducted in early July and June, such as Slovenia, Norway, Poland, and the United Kingdom, we examined the relationships between year-specific CDI and irrigation percentage to determine the appropriate irrigation reference year. A correct reference year is in particular relevant when correlating reported irrigated area with drought information obtained from GCWM.

Crop drought index (CDI)

The global crop water model - GCWM[31,32] was employed to compute crop water use (CWU, m^3) based on a daily soil water balance considering evapotranspiration, precipitation, runoff, and irrigation. The CWU includes green (CWU_G) and blue crop water use (CWU_B). CWU_B is the amount of evapotranspiration on cropland stemming from irrigation; CWU_G is the fraction of in-situ rainfall that infiltrates into the soil and is available for crops. For irrigated crops, the crop evapotranspiration is assumed at the potential level (PET_c, mm day^{-1}) which is the maximum daily evapotranspiration of crops under healthy and well-watered conditions, impacted by specific crop type and phenological phases of crops. PET_c is calculated by multiplying reference evaporation (ET_0, mm day^{-1}) with a crop coefficient. The GCWM adopts the FAO Penman-Monteith method[50] to calculate ET_0. CWU_G of irrigated crops is set to the actual evapotranspiration of crops (AET_c), which would be observed without irrigation. CWU_B of irrigated crops is set to the difference between PET_c and its CWU_G. CDI is calculated as

$$\mathrm{CDI} = 1 - \frac{\mathrm{CWU_G\_Y}/(\mathrm{CWU_G\_Y} + \mathrm{CWU_B\_Y})}{\mathrm{CWU_G\_LT}/(\mathrm{CWU_G\_LT} + \mathrm{CWU_B\_LT})} = 1 - \frac{\mathrm{AET_c\_Y}/\mathrm{PET_c\_Y}}{\mathrm{AET_c\_LT}/\mathrm{PET_c\_LT}} \quad (1)$$

Where Y is the specific year Y; LT is the reference time period 1986–2015; AET_c_Y is the actual evapotranspiration of irrigated crops in the year Y, and AET_c_LT is the average actual evapotranspiration of irrigated crops for the period 1986–2015. For CDI calculation, the annual total of CWU, AET, and PET for all 26 crop groups was computed. CDI reflects therefore the drought condition in a specific year compared to the drought condition in the reference period 1986–2015. Positive values of CDI indicate that the conditions in the year Y are dryer than on average in the long-term reference period, whereas negative CDI values indicate wet years.

The spatial resolution of GCWM simulation results is 5 arc min. GCWM inputs include the cropping pattern and cropping season, climate, and soil conditions. Monthly growing areas and cropping seasons were obtained from the MIRCA2000 dataset[17], covering the growing area of 26 crop classes (all major food crops, cotton, and other unspecified perennial, annual, and fodder grasses) and their corresponding growing period from the start of cultivation to harvest months in the year 2000 (center of reference period), distinguishing irrigated and rainfed crops. MIRCA2000 represents multiple-cropping systems and maximizes the agreement with national and subnational statistical surveys. The gridded daily climate and soil data are derived from ERA5 global reanalysis[51] and ISRICWISE30sec v1.0[52], respectively. The gridded CDI was transferred to NUTS levels by calculating the harvested area weighted average values of CDI for all pixels within each NUTS unit.

Developing AEI time series

The simple approach for developing the AEI time series involved employing linear interpolation of the reported AEI (about 10–12 sample years, Fig. 1 and Supplementary A Table S2). For instance, if AEI values were reported in 2010 and 2013, those for 2011 and 2012 were estimated using the linear interpolation between data in 2010 and 2013. To extrapolate AEI data prior to and after the years for which AEI values were available, the values from the nearest year were utilized. For example, if the earliest reported AEI was in 1995, AEI for the years 1990–1994 was assumed to be the same as that for 1995; similarly, if the latest reported AEI was in 2016, AEI for 2017–2020 was assumed to be the same as that for 2016. This approach resulted in the development of Dataset 1.

However, AEI change is expected to be a gradual trend rather than abrupt fluctuations, as irrigation facilities do not tend to disappear or reappear suddenly within short periods. Nevertheless, reported data reveals that some AEI values undergo notable and abrupt variations such as in Austria and the UK, possibly due to inconsistencies during data collection and statistical processing, as well as the influences of AEI definition. For example, the AEI definition in Austria considers irrigation equipment and water resource availability; Poland neglected the farmland with a size of less than 20 ha; Switzerland defined AEI as irrigated area in the dry year 2006. To alleviate this issue, the advanced approach – data filtering and spline interpolation – is adopted for generating annual AEI time series (Dataset 3, smoothed AEI). We applied a filter to exclude only those AEI values that were lower than expected. Specifically, the reported AEI is filtered using the following approach:

$$\mathrm{AEI}_{\mathrm{expect},i} = ai + b \quad (2)$$

$$\gamma = k \cdot \mathrm{AEI}_{\mathrm{expect},i} \quad (3)$$

Where $AEI_{expect,\ i}$ is the expected AEI in the year i. The coefficients a and b are determined based on the AEI values from the preceding and subsequent years. We conducted tests on k ranging from 0.70 to 0.95, with increments of 0.05. The default coefficient k is set to 0.85 after visually inspecting with a particular focus on regions experiencing notable AEI changes, and ensuring an adequate number of AEI records for spline smoothing. Generally, for subnational regions within a country, their k values are assumed to be the same. However, due to AEI data features (such as impacts by historical factors in Central and Eastern European countries) and the limitation of data availability, the k values of these NUTS units were adjusted. The γ is the threshold for AEI filtering; the AEI value in the year i will be filtered if it is lower than γ. Details of generating dynamic AEI datasets are shown in Supplementary Data C1.

Following the AEI data filtering, the spline interpolation is conducted to obtain smoothed AEI (Dataset 3) using the *smooth.spline* function in R 4.2.0. In this smooth function, the parameter *spar* is the smoothing parameter that controls the degree of smoothness, with larger values leading to smoother curves while smaller values result in more detailed curves. A default value of 0.45 is used after several trials.

Developing AAI time series and calculating AAI anomaly

Our essential assumption is that the interannual variation of irrigation percentage is influenced by wet and dry climate conditions characterized by CDI. Therefore, the estimation of dynamic AAI data was established by using the AEI time-series, and the correlations between CDI and reported irrigation percentage as follows (Fig. 1):

$$\frac{AAI_i}{AEI_i}(\%) = \beta_0 + \beta_1 \times CDI_i \quad (4)$$

Where AEI_i is the smoothed AEI in the year i (annual, 1990–2020, Dataset 3); AAI_i is the estimated AAI in the year i (annual, 1990–2020); β_0 and β_1 are coefficients (shown in Supplementary Data C2) calculated from the ordinary least square linear regressions between CDI and reported irrigation percentage (about 5–8 sample years). One strategy involved calculating reported irrigation percentage via the percentage of reported AAI to reported AEI, adhering to the reported irrigation percentage, resulting in Dataset 4 (Fig. 1). Another strategy calculated reported irrigation percentage via the percentage of reported AAI to smoothed AEI, aiming to mitigate potential biases in the reported AEI from issues such as varying definitions across regions, resulting in Dataset 5 (Fig. 1). Dataset 6, representing the best guess AAI, was derived from the comparison of Datasets 4 and 5 by evaluating their correlation values (r) between CDI and reported irrigation percentage with corresponding significance levels, and the relative root mean square error (RRMSE, ha) between estimated and reported AAI. Generally, we prefer AAI estimated using the AAI/reported AEI strategy (Dataset 4), unless the AAI/smoothed AEI strategy (Dataset 5) performs obviously better (AAI selection for Dataset 6 is in Supplementary Data C2). Above AAI Datasets 4–6 were generated using the advanced approach, while Dataset 2 was created through the simple method (the same as that for AEI in Dataset 1) of the reported AAI.

Furthermore, due to the conversion of political systems in Eastern European socialist countries, they possessed a considerable number of large-scale irrigation facilities in the early 1990s. However, these facilities gradually ceased operation, leading to drastic changes in irrigation[30]. To establish robust relationships between CDI and irrigation percentage, we undertook a temporal partitioning of irrigation data processing for Romania. This involved separating the data into periods before 2010 reflecting declining irrigation extent and after 2010 reflecting a partial rehabilitation after the transition (Supplementary Data C2).

To show the variations in AAI time series across regions and identify years with obviously higher or lower irrigated areas than expected, we calculated the relative AAI anomalies. Specifically, the AAI time series derived from the advanced approach (Dataset 6) underwent Min-Max normalization, with values ranging from 0 to 1. Subsequently, spline interpolation was applied to the relative AAI for each region to obtain the smoothed trendline, using the *smooth.spline* function in R 4.2.0 with a spar value of 0.45 (same as the AEI smoothing). The anomaly of relative AAI was calculated as the difference between the smoothed trendline and the relative AAI. Therefore, the anomalies of relative AAI represent the differences introduced by considering the impacts of dry and wet conditions on AAI (Fig. 4a and Fig. 5a–d).

Assessment of generated irrigation datasets

The assessment focuses on Datasets 3 and 6 - dynamic AEI from data filtering and spline smoothing and best-guess AAI generated using the advanced approach, as they provide annual dynamics and potentially more accurate irrigation information, and these two datasets were recommended for application. Given that all reported irrigation data were used for data generation, this study utilized remote sensing products and Land Use/Cover Area frame statistical Survey (LUCAS) data to evaluate the generated irrigation dataset.

The LUCAS survey divided regions into 2 km x 2 km grids, conducting a point-level field observation within each grid for the years 2006, 2009, 2012, 2015, and 2018, independent from our datasets. To align LUCAS with our data, we converted the point-level information into subnational levels. The original LUCAS points were firstly filtered based on specific water management (WM) series, including irrigation (1), potential irrigation (2), drainage (3), irrigation and drainage (4), no visible water management (5), and not relevant (8). We focused on WM codes 1–5, isolating irrigation-related points (8) in farmland. Then, we confirmed the land use and cover labels of these points were related to agricultural land use and covered by crops.

Due to no available irrigation data in 2006 and limited irrigation information in subnational LUCAS surveys, we compared our irrigation area datasets with LUCAS at the country level for the years 2009, 2012, 2015, and 2018. Countries with fewer than 30 irrigable points were excluded. Since converting LUCAS point data to irrigation extent was impractical, we compared the irrigation percentage of two datasets. The irrigation percentage for LUCAS data (AAI/AEI_LUCAS, %) is calculated as follows,

$$AAI/AEI\_LUCAS(\%) = 100\% \times n_{irrigated}/n_{irrigable} \quad (5)$$

Where $n_{irrigated}$ is the count of points that are irrigated, equal to the sum of points categorized under WM codes 1 and 4; $n_{irrigable}$ is the count of irrigable points, encompassing the sum of points under WM codes 1, 2, and 4. The spatial distribution of LUCAS irrigable and irrigated points is shown in Supplementary A Fig. S7.

Challenges arose in remote sensing-derived irrigation products due to limitations in comprehensive datasets covering time and regions. Our comparisons were conducted regionally or for specific time frames. We chose three global remote sensing-derived irrigation area-specific datasets—GIAM[16], GRIPC[19], and GMIE[21]. While GIAM is exclusively derived from remote sensing, GRIPC and GMIE incorporate survey data to some extent. Details for the above remote sensing datasets are outlined in Supplementary E.

Data availability

The ELIAD dataset, supplementary materials, and the data used for figures and tables (Supplementary Data F) in the manuscript are available open-access at https://doi.org/10.5281/zenodo.10715269.

Received: 20 March 2024; Accepted: 23 September 2024;
Published online: 03 October 2024

References

1. D'Odorico, P. et al. The Global Food-Energy-Water Nexus. *Rev. Geophys.* **56**, 456–531 (2018).

2. Karthikeyan, L., Chawla, I. & Mishra, A. K. A review of remote sensing applications in agriculture for food security: Crop growth and yield, irrigation, and crop losses. *J. Hydrol.* **586**, 124905 (2020).
3. Grafton, R. Q. et al. Global insights into water resources, climate change and governance. *Nat. Clim. Change* **3**, 315–321 (2013).
4. Zhao, G. et al. The implication of irrigation in climate change impact assessment: a European-wide study. *Global Change Biol* **21**, 4031–4048 (2015).
5. Zajac, Z. et al. Estimation of spatial distribution of irrigated crop areas in Europe for large-scale modelling applications. *Agr. Water Manage.* **266**, 107527 (2022).
6. Wriedt, G., Van der Velde, M., Aloe, A. & Bouraoui, F. Estimating irrigation water requirements in Europe. *J. Hydrol.* **373**, 527–544 (2009).
7. Wriedt, G., van der Velde, M., Aloe, A. & Bouraoui, F. A European irrigation map for spatially distributed agricultural modelling. *Agr. Water Manage.* **96**, 771–789 (2009).
8. Iglesias, A. & Garrote, L. Adaptation strategies for agricultural water management under climate change in Europe. *Agr. Water Manage.* **155**, 113–124 (2015).
9. Tramblay, Y. et al. Challenges for drought assessment in the Mediterranean region under future climate scenarios. *Earth-Sci. Rev.* **210**, 103348 (2020).
10. Elliott, J. et al. Constraints and potentials of future irrigation water availability on agricultural production under climate change. *P. Nal. A. Sci.* **111**, 3239–3244 (2014).
11. Pereira, L. S., Paredes, P. & Jovanovic, N. Soil water balance models for determining crop water and irrigation requirements and irrigation scheduling focusing on the FAO56 method and the dual Kc approach. *Agr. Water Manage.* **241**, 106357 (2020).
12. Cancela, J. J., Cuesta, T. S., Neira, X. X. & Pereira, L. S. Modelling for Improved Irrigation Water Management in a Temperate Region of Northern Spain. *Biosyst. Eng.* **94**, 151–163 (2006).
13. Puy, A., Borgonovo, E., Lo Piano, S., Levin, S. A. & Saltelli, A. Irrigated areas drive irrigation water withdrawals. *Nat. Commun.* **12**, 4525 (2021).
14. Dari, J. et al. Regional data sets of high-resolution (1 and 6 km) irrigation estimates from space. *Earth Syst. Sci. Data* **15**, 1555–1575 (2023).
15. Xie, Y. & Lark, T. J. Mapping annual irrigation from Landsat imagery and environmental variables across the conterminous United States, 1997-2017. *Remote Sens. Environ.* **260**, 112445 (2021).
16. Thenkabail, P. S. et al. Global irrigated area map (GIAM), derived from remote sensing, for the end of the last millennium. *Int. J. Remote Sens.* **30**, 3679–3733 (2009).
17. Portmann, F. T., Siebert, S. & Döll, P. MIRCA2000—Global monthly irrigated and rainfed crop areas around the year 2000: A new high-resolution data set for agricultural and hydrological modeling. *Global Biogeochem. Cy.* **24**, GB1011 (2010).
18. Siebert, S. et al. A global data set of the extent of irrigated land from 1900 to 2005. *Hydrol. Earth Syst. Sc.* **19**, 1521–1545 (2015).
19. Salmon, J. M., Friedl, M. A., Frolking, S., Wisser, D. & Douglas, E. M. Global rain-fed, irrigated, and paddy croplands: A new high resolution map derived from remote sensing, crop inventories and climate data. *Int. J. Appl. Earth Obs.* **38**, 321–334 (2015).
20. Meier, J., Zabel, F. & Mauser, W. A global approach to estimate irrigated areas – a comparison between different data and statistics. *Hydrol. Earth Syst. Sci.* **22**, 1119–1133 (2018).
21. Wu, B. et al. Mapping global maximum irrigation extent at 30m resolution using the irrigation performances under drought stress. *Global Environ. Chang.* **79**, 102652 (2023).
22. EUROSTAT. Irrigation: number of farms, areas and equipment by size of irrigated area and NUTS 2 regions. https://doi.org/10.2908/EF_POIRRIG (2018). (Accessed in March 2023).
23. EUROSTAT. Irrigation of agricultural holdings. https://doi.org/10.2908/EF_MP_IRRI (2020). (Accessed in March 2023).
24. EUROSTAT. Land use: number of farms and areas by size of farm (UAA) and LFA status. https://doi.org/10.2908/EF_OV_LUSUM (2009) (Accessed in March 2023).
25. Jalilvand, E., Tajrishy, M., Ghazi Zadeh Hashemi, S. A. & Brocca, L. Quantification of irrigation water using remote sensing of soil moisture in a semi-arid region. *Remote Sens. Environ.* **231**, 111226 (2019).
26. Zhang, L., Zhang, K., Zhu, X., Chen, H. & Wang, W. Integrating remote sensing, irrigation suitability and statistical data for irrigated cropland mapping over mainland China. *J. Hydrol.* **613**, 128413 (2022).
27. Dari, J. et al. Detecting and mapping irrigated areas in a Mediterranean environment by using remote sensing soil moisture and a land surface model. *J. Hydrol.* **596**, 126129 (2021).
28. Lawston, P. M., Santanello, J. A. & Kumar, S. V. Irrigation Signals Detected From SMAP Soil Moisture Retrievals. *Geophys. Res. Lett.* **44**, 11860–11867 (2017).
29. Chen, Y. et al. Detecting irrigation extent, frequency, and timing in a heterogeneous arid agricultural region using MODIS time series, Landsat imagery, and ancillary data. *Remote Sens. Environ.* **204**, 197–211 (2018).
30. Zhovtonog, O., Dirksen, W. & Roest, K. Comparative assessment of irrigation sector reforms in Central and Eastern European countries of transition. *Irrig. Drain.* **54**, 487–500 (2005).
31. Meza, I. et al. Drought risk for agricultural systems in South Africa: Drivers, spatial patterns, and implications for drought risk management. *Sci. Total Environ.* **799**, 149505 (2021).
32. Siebert, S. & Döll, P. Quantifying blue and green virtual water contents in global crop production as well as potential production losses without irrigation. *J. Hydrol.* **384**, 198–217 (2010).
33. Rosa, L., Chiarelli, D. D., Rulli, M. C., Dell'Angelo, J. & D'Odorico, P. Global agricultural economic water scarcity. *Sci. Adv.* **6**, eaaz6031 (2020).
34. Wada, Y., van Beek, L. P. H. & Bierkens, M. F. P. Modelling global water stress of the recent past: on the relative importance of trends in water demand and climate variability. *Hydrol Earth Syst. Sc.* **15**, 3785–3808 (2011).
35. Harmanny, K. S. & Malek, Ž. Adaptations in irrigated agriculture in the Mediterranean region: an overview and spatial analysis of implemented strategies. *Reg. Environ. Change* **19**, 1401–1416 (2019).
36. Buras, A., Rammig, A. & Zang, C. S. Quantifying impacts of the 2018 drought on European ecosystems in comparison to 2003. *Biogeosciences* **17**, 1655–1672 (2020).
37. Ospina, R. & Marmolejo-Ramos, F. Performance of Some Estimators of Relative Variability. *Front. Appl. Math. Stat.* **5**, 43 (2019).
38. Dari, J. et al. Exploiting High-Resolution Remote Sensing Soil Moisture to Estimate Irrigation Water Amounts over a Mediterranean Region. *Remote Sens* **12**, 2593 (2020).
39. Zhu, X., Zhu, W., Zhang, J. & Pan, Y. Mapping Irrigated Areas in China From Remote Sensing and Statistical Data. *IEEE J-STARS* **7**, 4490–4504 (2014).
40. Ambika, A. K., Wardlow, B. & Mishra, V. Remotely sensed high resolution irrigated area mapping in India for 2000 to 2015. *Sci Data* **3**, 160118 (2016).
41. Zhang, C., Dong, J., Xie, Y., Zhang, X. & Ge, Q. Mapping irrigated croplands in China using a synergetic training sample generating method, machine learning classifier, and Google Earth Engine. *Int. J. Appl. Earth Obs.* **112**, 102888 (2022).
42. Ajaz, A., Karimi, P., Cai, X., De Fraiture, C. & Akhter, M. S. Statistical Data Collection Methodologies of Irrigated Areas and Their Limitations: A Review. *Irrig. Drain.* **68**, 702–713 (2019).
43. Alcantara, C. et al. Mapping the extent of abandoned farmland in Central and Eastern Europe using MODIS time series satellite data. *Environ. Res. Lett.* **8**, 035035 (2013).

44. Ronco, P. et al. A risk assessment framework for irrigated agriculture under climate change. *Adv. Water Resour.* **110**, 562–578 (2017).
45. Yu, Q. et al. A cultivated planet in 2010 – Part 2: The global gridded agricultural-production maps. *Earth Syst. Sci. Data* **12**, 3545–3572 (2020).
46. Metzger, M. J., Bunce, R. G. H., Jongman, R. H. G., Mücher, C. A. & Watkins, J. W. A climatic stratification of the environment of Europe. *Global Ecol. Biogeogr.* **14**, 549–563 (2005).
47. Xie, Y., Gibbs, H. K. & Lark, T. J. Landsat-based Irrigation Dataset (LANID): 30 m resolution maps of irrigation distribution, frequency, and change for the US, 1997–2017. *Earth Syst. Sci. Data* **13**, 5689–5710 (2021).
48. Vanschoenwinkel, J., Vancauteren, M. & Van Passel, S. How do western european farms behave and respond to climate change? a simultaneous irrigation-crop decision model. *Clim. Change Econ.* **13**, 2250009 (2022).
49. EUROSTAT. Nuts - nomenclature of territorial units for statistics. https://ec.europa.eu/eurostat/de/web/nuts (2023) (Accessed in March 2023).
50. Allen, R. G., Luis S. P., Raes, D. & Smith, M. *FAO Irrigation and Drainage Paper*. https://www.fao.org/4/T0231E/t0231e0c.htm (1998).
51. Hersbach, H. et al. The ERA5 global reanalysis. *Q. J. Roy. Meteor. Soc.* **146**, 1999–2049 (2020).
52. Batjes, N. H. Harmonized soil property values for broad-scale modelling (WISE30sec) with estimates of global soil carbon stocks. *Geoderma* **269**, 61–68 (2016).

Acknowledgements

This study is funded by the Deutsche Forschungsgemeinschaft (DFG, German Research Foundation) – SFB 1502/1–2022 - Projektnummer: 450058266. We acknowledge support by the Open Access Publication Funds of the Göttingen University. The authors would like to thank the scientific programmr Malte Weller (University of Göttingen) for performing the GCWM simulations and for help with data processing. We also appreciate the supports and helpful suggestions from CRC DETECT members.

Author contributions

W.Z. created the dataset and wrote the original manuscript draft. S.S. proposed the research idea. Both authors jointly developed the methodology and reviewed and edited the manuscript.

Funding

Open Access funding enabled and organized by Projekt DEAL.

Competing interests

The authors declare no competing interests.

Additional information

Supplementary information The online version contains supplementary material available at https://doi.org/10.1038/s43247-024-01721-z.

Correspondence and requests for materials should be addressed to Wanxue Zhu.

Peer review information *Communications Earth & Environment* thanks Emiliano Gelati and Luca Brocca for their contribution to the peer review of this work. Primary Handling Editors: Heike Langenberg. A peer review file is available.